

Design and Safety Aspects of a Collaborative Robotics Application for the Disassembly of Exhausted BEV Batteries

*Original*

Design and Safety Aspects of a Collaborative Robotics Application for the Disassembly of Exhausted BEV Batteries / Salamina, L., Calvo, G., Ferraro, A., Gaidano, M., Melchiorre, M., Mauro, S.. - ELETTRONICO. - (2024), pp. 1-9. (ASME 2024 International Mechanical Engineering Congress and Exposition Portland, OR (USA) November 17-21, 2024) [10.1115/IMECE2024-145504].

*Availability:*

This version is available at: 11583/2995964 since: 2024-12-27T15:11:51Z

*Publisher:*

ASME

*Published*

DOI:10.1115/IMECE2024-145504

*Terms of use:*

This article is made available under terms and conditions as specified in the corresponding bibliographic description in the repository

*Publisher copyright*

AIAA preprint/submitted version e/o postprint/Author's Accepted Manuscript

(Article begins on next page)

## DESIGN AND SAFETY ASPECTS OF A COLLABORATIVE ROBOTICS APPLICATION FOR THE DISASSEMBLY OF EXHAUSTED BEV BATTERIES

Laura Salamina<sup>1</sup>, Giulia Calvo<sup>1</sup>, Alessandra Ferraro<sup>2</sup>, Matteo Gaidano<sup>1</sup>, Matteo Melchiorre<sup>1</sup>, and Stefano Mauro<sup>1</sup>

1 – Politecnico di Torino, Department of Mechanical and Aerospace Engineering

2 – INAIL, DIT Department, Roma, Italy

### ABSTRACT

*The recycling of used vehicle batteries represents a key challenge for the sustainability of the electrification process of road transport. The process involves two distinct phases: the first consists of the disassembly of the battery pack and the separation of its components and the lithium cells that make up its basic elements, while the second involves the recovery of the basic elements in waste treatment plants. The first phase requires the implementation of a sequence of disassembly operations that vary for each type of battery pack to be recovered.*

*In this work, we investigate the possibility of using a collaborative robotic cell for this first phase, in which a human operator carries out the disassembly operations with the help of an anthropomorphic robot installed on a mobile base, which is thus able to reach any point on the battery by moving appropriately around the work surface.*

*The disassembly cycle of a well-known battery is analyzed. This first analysis shows that in order to reduce the time required to complete the operation, it is necessary for man and robot to perform certain operations by sharing the work space.*

*The second part of the article then introduces collision avoidance algorithms for robots that allow them to share the workspace in compliance with current technical regulations.*

*The results obtained are illustrated by means of simulations carried out in a mixed simulation environment.*

Keywords: electric waste recycling, collaborative robotics, safety

### 1. INTRODUCTION

The worldwide energy transition aimed at reducing CO<sub>2</sub> emissions involves the electrification of most systems, particularly road transport. The technologically most widespread solution to date involves the use of batteries, in most cases lithium, while alternative solutions such as the use of hydrogen,

for example, may possibly become more widespread in the future [1].

Therefore, the need to recycle end-of-life batteries has already arisen and will undoubtedly increase in the future, with the twofold aim of minimizing the landfilling of spent components and recovering valuable raw materials, primarily lithium [1].

The recycling of vehicle batteries can be carried out according to different strategies, based on the residual charge capacity: if this exceeds 75%, the entire battery pack can be reused for static applications [2], such as storage for renewable energy plants, while otherwise the battery pack will have to be disassembled until the individual cells are separated, and then those that are still in good condition can be reused for the assembly of new batteries, while those that are definitively exhausted will have to be crushed and recovered in a chemical plant [4].

The dismantling of batteries is a particular application case of technologies dedicated to the recovery waste from electrical and electronic equipment (WEEE), which still requires major technological developments to be carried out by robot systems [3]. A specific approach to the recycling of automotive electrical and electronic components is proposed in Li's work [4], [5]. Marconi et al. proposed a robotic system for dismantling electronic boards [6]. Ruggeri in his work [7] emphasises that the collaboration between the expertise of the human operator and the precision of robots may be the best solution for an effective disassembly of electronic components. Chatzikonstantinou[8] and Li [9] analyse possible ways of collaboration between humans and robots for disassembly, focusing in particular on the ergonomics of the process. Alvarez [10] and Renteria [11] confirm with their studies that the disassembly of electronic components by means of collaborative robotics applications increases the economic yield of the process and its safety.

The development of effective ways of human-robot collaboration involves the development of algorithms for

interaction through direct contact and force exchange between man and robot [12]. Methods based on the use of vision systems that detect the position of the operator can also be very useful, [13] which can be used to avoid collisions [14] or to perform handover operations [15]. In addition, methods for monitoring the operator [16] and for checking the health of the robot [17] or its components [18] may be applied to improve safety at work.

In this work, the disassembly phase of the battery is analysed with the aim of separating the battery modules and the cells within them in order to subsequently send them for recovery in dedicated facilities or, if the possibility exists, for direct reuse of the cells that are still suitable for use.

The article in the following describes the approach used to study a flexible robot cell, capable of operating on large batteries, allowing the actions of a human operator and those of a 7-axis collaborative robot installed on a mobile platform to be coordinated. The results obtained in [2] and [19] are applied and adapted to this process.

First of all, the battery disassembly process is analysed and a suitable sequence of operations is identified to keep the time required within acceptable limits, highlighting in which cases the operator and robot share the work space.

## 2. DISASSEMBLY CYCLE ANALYSIS

The system proposed in this paper was developed using the disassembly of the battery of a 2017 mid-size electric vehicle as a reference operation, for which there is plenty of information available in the literature [21]. The battery is 1600 mm long and 1000 mm wide. It consists of 10 modules, divided into five sections. A total of 76 parts and 374 fasteners were identified.

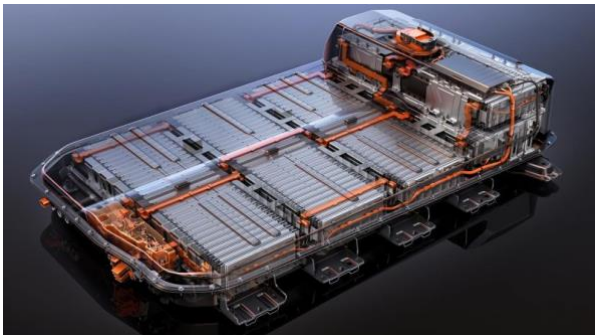


**FIGURE 1** BATTERY CONSIDERED FOR DISASSEMBLY [21]

For a generic battery, the main actions for disassembly can be summarised as follows:

- remove the cover
- separate the battery modules from the other electrical components
- mechanically disconnect the battery modules and electrical components from the battery base
- remove electrical components
- remove battery modules
- disassemble the individual battery modules

The disassembled battery is shown in FIGURE 1. Its disassembly cycle is analyzed and described in detail in [20]. There are 46 disassembly steps identified, and it is possible to identify a priority table that defines which steps must necessarily be performed in a predefined sequence and which can be performed independently, without the need for a specific sequence.

For the purpose of defining the disassembly cycle to be implemented, each operation was also analysed in order to define on the basis of its complexity whether or not it can be advantageously performed by a robot.

By analysing each operation, it is therefore possible to assess whether it can be carried out by a robot or whether it should be done by a human operator. It is also possible to assess the time required to carry out the individual step by an operator or by the robot. This information is then used to analyse the possible processing sequences in order to calculate the total disassembly time of the battery following the different possible options. The analysis is conducted under the assumption that a human operator and a robot operate simultaneously, with the human operator preferably performing actions identified as only executable by humans.

The data entered in an analysis software written by the authors allows the calculation of the time required to perform a given disassembly sequence, while at the same time providing an indication of the time phases in which man and robot operate in the same work space, thus making it necessary to adopt methodologies and algorithms that guarantee safety in the sharing of space between man and robot.

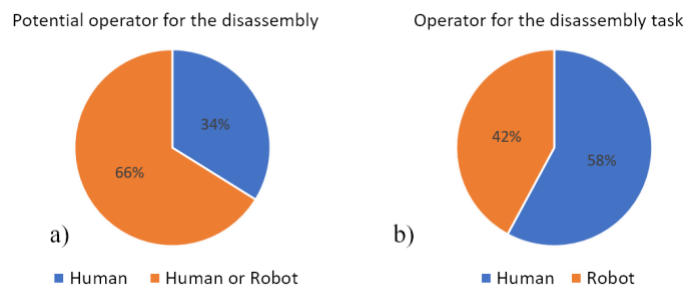


**FIGURE 2** OPERATOR FOR THE DISASSEMBLY SEQUENCE

FIGURE 2 shows the results of the analysis of the disassembly tasks, in a), and of a possible disassembly sequence, in b). b) shows that, in a possible disassembly sequence, the 58% of the tasks is performed by the human and the 42% is performed by the robot.

FIGURE 3 shows the results of the disassembly time calculation obtained according to different sequences.

The choice of the best sequence allows the battery to be disassembled in about 3580 s, while the worst sequence requires 3850 s for the process to be completed, a time aggravation of about 7%.

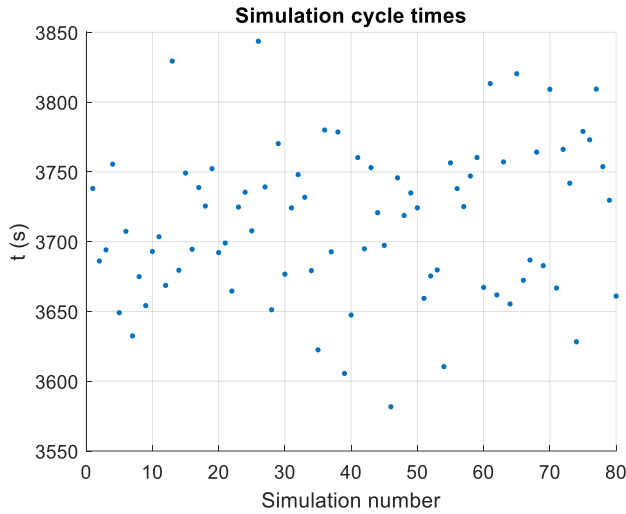


**FIGURE 3** DISASSEMBLY TIME WITH DIFFERENT SEQUENCES

FIGURE 4 shows the GANTT diagram of the best sequence identified. Indicated in green is the time during which operations are carried out, in blue that for tool change, in yellow that for movement, in red the interference time and in white any waiting time for synchronisation between man and robot.

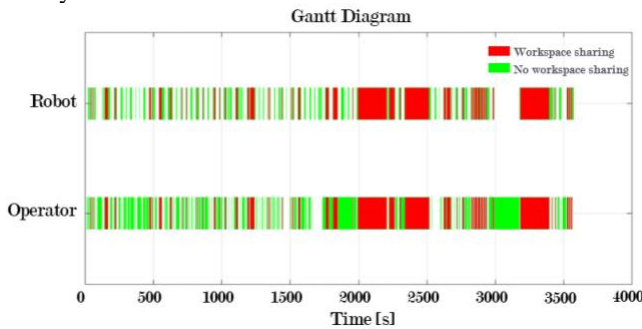


**FIGURE 4** GANTT DIAGRAM OF DISASSEMBLY OPERATIONS

In the steps highlighted in red, algorithms must be implemented to ensure security in workspace sharing

### 3. ROBOTIC SYSTEM MODELLING

In order to support the human operator in battery disassembly operations, the use of a robot system consisting of a seven-axis Franka Emika collaborative robot installed on a Tiago mobile base manufactured by PAL Robotics is considered. This solution provides a system capable of performing disassembly operations regardless of the size of the battery. The battery being disassembled rests on a workbench and the tools required to

perform all operations are available at its side. The system consisting of the anthropomorphic robot and the mobile base is a complex robot, with a total of ten degrees of freedom, whose detailed dynamic model is similar to that described in [22].

The system described is simulated in the CoppeliaSim environment; the kinematic models of the two robots involved, the static model of the battery being disassembled and a kinematic model of a human operator, represented by means of a complete mannequin, equipped with all its limbs, were developed.

In order to carry out simulations suitable for verifying the potential effectiveness of the human-robot interaction algorithms under development, the operator is made to perform certain movements according to pre-set sequences and the ability of the algorithms to modify the robot's trajectory in order to avoid colliding with the operator, to maintain distances in compliance with regulations and to carry out the task in any case, provided that access to the work area is not completely precluded by the presence of the operator.

The simulation environment developed interacts with a calculation environment implemented in Matlab. The Matlab code determines the trajectories followed by the operator and the robot, while the CoppeliaSim environment makes it possible to easily represent the positions reached and to measure relative distances and speeds between the elements represented, and thus in particular between man, robot, workbench and battery.

FIGURE 5 shows a picture of the simulated environment.

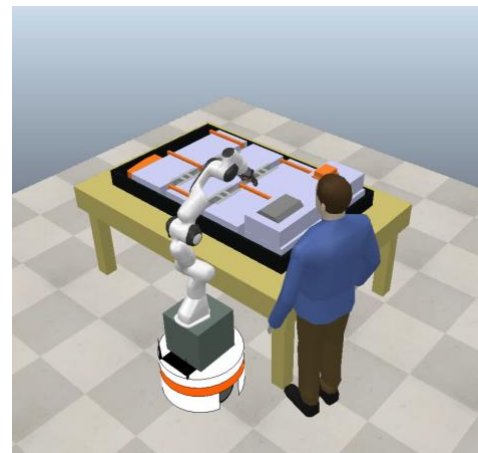


**FIGURE 5** SIMULATED ENVIRONMENT

### 4. COLLISION AVOIDANCE ALGORITHM

In order to make collaboration between man and robot possible, and in particular the sharing of the work space, algorithms have been designed and implemented to modify the trajectory of the mobile base and the anthropomorphic robot in real time so as to prevent collision in any case and to comply with the provisions of standard ISO/TS 15066.

This standard requires that in shared workspace conditions, where there is no contact between man and robot, the minimum

distance to be respected between them is determined as a function of the speed of the man and robot as well as the robot's reaction time and its maximum acceleration. This distance is defined as

$$d_{min} = (v_m + v_r)T_r + \frac{v_r^2}{2a_s} \quad (1)$$

where  $v$  denotes speed,  $T$  the reaction time,  $a_s$  the deceleration. The subscripts  $m$  and  $r$  refer to the human operator and the robot respectively.

Two different algorithms were developed based on the virtual potentials method, one aimed at generating trajectories for the mobile base and the second for generating trajectories for the anthropomorphic robot.

In both cases, it is assumed that, in the real case scenario, a set of sensors makes available the position information of the human operator. It is also assumed that the guidance algorithms of the mobile base allow the pose of the mobile base to be known with an accuracy of less than 10 mm, while the pose of all links of the anthropomorphic robot is assumed to be known by combining the pose data of the mobile base with the rotation angles of the joints.

## 5. COLLISION AVOIDANCE ALGORITHM FOR MOBILE BASE

For the purposes of the development of the guidance algorithm for the mobile base, it is considered that this will have to be able to guide the base towards the working position envisaged in the disassembly cycle and to orient it appropriately, avoiding any collision with the human operator and the surrounding environment, in this case considered exclusively as the work surface on which the battery is positioned.

For the purposes of defining the virtual potential fields associated with the operator and the work surface, a simplified geometry is therefore considered: the table is defined as a sigmoidal surface that includes it, while the human is considered to be included in a cylinder-shaped surface whose axis is centred on the axis of the operator's torso. The simplification of the geometry assumed to represent the space interdicted to the robot in order to avoid collision with the operator makes it possible to contain calculation times and to make the algorithm compatible with the use of sensors typically installed on board the platform, such as LIDAR and cameras.

The virtual potential field associated with the operator is defined as:

$$U_m(x, y) = K_m e^{-\frac{\gamma m}{2}((x_b - x_m)^2 + (y_b - y_m)^2)} \quad (2)$$

While the one associated with the workspace is:

$$U_t = K_t \prod_{i=1}^4 \frac{1}{1 + e^{-\gamma_t(A_i(x_b - x_t) + B_i(y_b - y_t) + C_i)}} \quad (3)$$

Where the coefficient  $K$  defines the field strength and  $\gamma$  its decay. The coefficients  $A_i$ ,  $B_i$  and  $C_i$  allow the field to be given the desired shape. The subscripts  $b$ ,  $m$  and  $t$  refer to the moving base,

the circle representing the operator and the area occupied by the working plane.

FIGURE 6 and FIGURE 7 show the shapes obtained for the virtual potentials shaped according to Equations 2 and 3.

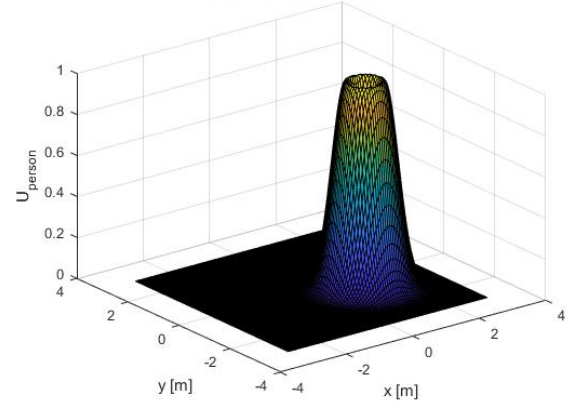


FIGURE 6 VIRTUAL POTENTIAL ASSOCIATED WITH THE OPERATOR

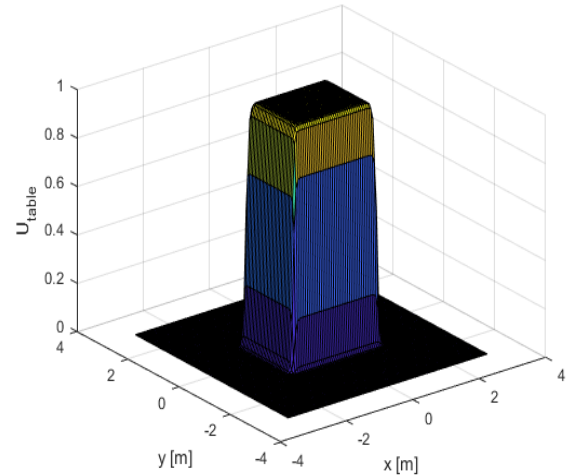


FIGURE 7 VIRTUAL POTENTIAL ASSOCIATED WITH THE WORK PLAN

The repulsive actions applied by the virtual potentials are calculated as the gradient of the potential field.

Finally, the target point  $P_a$  is associated with an attractive potential field  $U_a$  defined as:

$$U_a = \frac{\sigma}{2} |p_b - p_a|^2 \quad (4)$$

Where  $p_b = [x_b \ y_b]^T$  e  $p_a = [x_a \ y_a]^T$

The overall potential field used to define the velocity of the moving base at each instant is therefore given by the sum of the three potential fields defined by equations 2, 3 and 4

$$U = U_a + U_t + U_m \quad (4)$$

In which the  $U_t$  field is fixed while the  $U_a$  and  $U_m$  fields are updated at each interaction according to the definition of the position to which the mobile base must travel to perform the scheduled activity and the position assumed by the human operator.

At each instant, it is possible to calculate the desired direction for the speed of the mobile base as

$$\vec{\lambda} = \frac{-\nabla U}{|\nabla U|} \quad (5)$$

The velocity of the moving base is the sum of two terms, one attractive and one repulsive:

$$\vec{\lambda}_{at} = -\nabla U_a \quad (6)$$

$$\vec{\lambda}_r = -\nabla(U_t + U_m) \quad (7)$$

This calculation must be improved in order to optimise the path when more options are possible and to avoid that the presence of a local minimum of the overall potential field leads to the calculation of a velocity of zero and thus to the stopping of the moving base at a position other than the desired one.

The selection of the path is made on the basis of global navigation considerations: since the moving base must reach positions around a table, in each case the main movement requires circumnavigating the space occupied by the table. The movement can therefore be carried out according to a clockwise or counter-clockwise rotation; considering the current position of the base and the one to be reached, it is then immediate to evaluate which is the shortest path.

The angle between the segment joining the position of the mobile base centre of gravity to the geometric centre of the working plane and the segment joining the target position at this point indicates whether the clockwise or counter-clockwise path is shorter: simplifying the trajectory as circular, it will in fact be necessary to follow the path joining the two points according to an arc that subtends an obtuse angle. This reference indication is preserved for the determination of the direction of motion throughout navigation, and is used to define at each instant the base speed that would be followed by the moving base to reach the target position in the absence of other obstacles along the trajectory. Any local minimum points are overcome by considering the special case in which the velocity for the moving base, calculated as a function of the gradient of the potential

fields, is zero. This situation occurs in those cases where there is  $\vec{v}_{at} = -\vec{v}_r$ .

In this case we proceed by defining the ratio  $r = \frac{|\vec{v}_{at}|}{|\vec{v}_r|}$ ; at local minima this ratio is  $r=1$ . Furthermore, the versors  $\vec{\lambda}_{at}$  and  $\vec{\lambda}_r$  of the velocities  $\vec{v}_{at}$  and  $\vec{v}_r$  are such that  $\vec{\lambda}_{at} \cdot \vec{\lambda}_r = -1$ .

We then introduce a versor  $\vec{\lambda}_t$  perpendicular to  $\vec{\lambda}_{at}$  and  $\vec{\lambda}_r$ . Since the motion of the moving base occurs in the plane, only two possible verses can be selected; we proceed to identify the most appropriate one on the basis of the global navigation consideration set forth above.

Denoting by  $\phi$  the angle described to circumvent the obstacle in a counterclockwise direction, the matrix  $M$  is defined as:

$$M = \begin{cases} \begin{bmatrix} 0 & -1 \\ 1 & 0 \end{bmatrix}, & \phi \leq \pi \\ \begin{bmatrix} 0 & 1 \\ -1 & 0 \end{bmatrix}, & \phi > \pi \end{cases} \quad (8)$$

And it is determined:

$$\vec{\lambda}_t = M \vec{\lambda}_r \quad (9)$$

For values of  $r$  close to 1, the verse  $\vec{\lambda}_t$  identifying the direction of the moving base velocity is then defined as

$$\vec{\lambda} = \frac{r \vec{\lambda}_t + (1-r) \vec{\lambda}_a}{|r \vec{\lambda}_t + (1-r) \vec{\lambda}_a|} \quad (10)$$

## 6. COLLISION AVOIDANCE FOR FRANKA EMIKA ANTHROPOMORPHOUS ROBOT

The implementation of the collision avoidance algorithm for the guidance of the robotic arm follows the same basic concepts as for the mobile base, but in order to ensure safe interaction with humans, it is no longer sufficient to consider a cylindrical volume to represent the human's footprint. Furthermore, the actual geometry of the anthropomorphic robot is relatively complex, and taking this into account in a precise manner would excessively slow down any process of calculating distances between man and robot, making it effectively impossible to control the robot in real time.

To this end, it was decided to approximate man and robot by means of sets of bodies with simple geometry: the robot Franka Emika is considered as a set of 15 spheres positioned on its links, while man is represented as a set of 12 volumes with simple geometry such as spheres and cylinders.

FIGURE 8 and FIGURE 9 show how robot and man have been represented in simplified form.

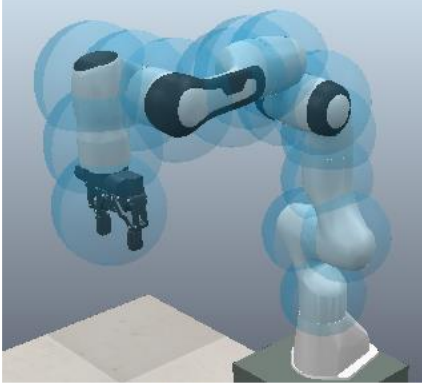


**FIGURE 8** ROBOT SCHEMATISATION USING SIMPLE GEOMETRY VOLUMES



**FIGURE 9** OPERATOR SCHEMATISATION USING SIMPLE GEOMETRY VOLUMES

The spheres are associated with the robot links according to **TABLE 1**.

**TABLE 1** ASSOCIATION BETWEEN SPHERES AND LINKS

SPHERE	1	2	3	4	5	6	7	8
LINK	1	1	2	2	3	3	4	4
SPHERE	<b>9</b>	<b>10</b>	<b>11</b>	<b>12</b>	<b>13</b>	<b>14</b>	<b>15</b>	
LINK	4	5	5	6	6	7	7	

The pose of each sphere can be calculated as a function of the coordinates  $q_i$  of each joint and the pose of the mobile base on which the robot is mounted.

Defined with  ${}^b\hat{A}_i = f(\mathbf{q})$  the matrix that defines the pose of the  $i$ -th sphere with respect to the mobile base, and with  ${}^0\hat{A}_b$  the matrix that determines the pose of the mobile base with respect to the fixed reference system, it is possible to know at every instant the pose of the  $i$ -th sphere as  ${}^0\hat{A}_i = {}^0\hat{A}_b {}^b\hat{A}_i$ , while the velocity of the  $i$ -th sphere is given by

$$\vec{v}_i = \vec{v}_b + \vec{\omega}_b \wedge \vec{p}_i + {}^0A_i {}^bJ_i \dot{q} \quad (11)$$

The maximum permissible speed  $v_{st}$  for each sphere at each instant is defined as a function of the distance between man and robot by Eq. 1.

Versor  $\vec{\lambda}_i = \frac{\vec{v}_i}{|\vec{v}_i|}$  defines the direction of the speed of the  $i$ -th sphere, while  $\vec{\lambda}_{ni}$  defines the common perpendicular between the  $i$ -th sphere and the closest solid representing the man.

Let  $v_{\lambda n, i}$  denote the component of the velocity of  $i$ -th sphere in the direction identified by  $\vec{\lambda}_{ni}$ .

A correction of the velocity of each closest sphere of the link is defined in order to respect the maximum velocity defined by ISO/TS 15066

$$v_{rep, i} = \begin{cases} v_{\lambda n, i} - v_{st} & \text{if } v_{st} \leq v_{\lambda n, i} \\ 0 & \text{if } v_{st} > v_{\lambda n, i} \end{cases} \quad (12)$$

This value is added to the reference velocity of the sphere and then it is converted in a velocity set for the joints of the robot, according to the technique applied in [23].

## 7. SIMULATION RESULTS

The algorithms presented in the previous paragraph were tested in the simulation environment in order to verify their effectiveness and assess their ability to generate trajectories suitable for avoiding collision with the human operator and reaching the position where the planned dismantling operation is to be carried out.

Two typical cases are considered:

- the mobile base describes a path that affects the space occupied by the operator and ends the run in an area where the anthropomorphic robot operates without interfering with humans
- the mobile base remains stationary, the anthropomorphic robot performs a disassembly operation sharing the workspace with the human operator

FIGURE 10 shows the initial and final positions of the robot and the operator in case a).

The trajectory followed by the moving platform to move from the initial to the final position is shown.

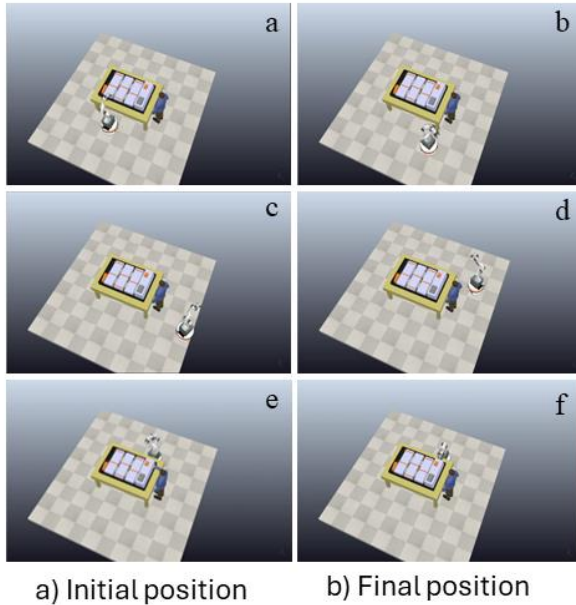


**FIGURE 10** MOBILE PLATFORM MOVEMENT, CASE a)

FIGURE 11 shows the relationship maintained during motion between the distance measured between the human and the robot and the speed maintained by the robot in its movement. The speed modulus is compared with the limit provided by the ISO/TS 15066 standard in relation to the distance between operator and robot. Only the maximum values measured are shown.

It can be seen that the speed obtained is always well below the value permitted by the standard.

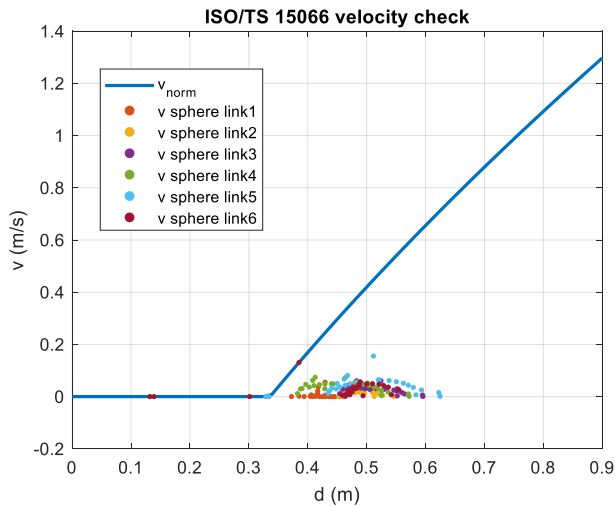
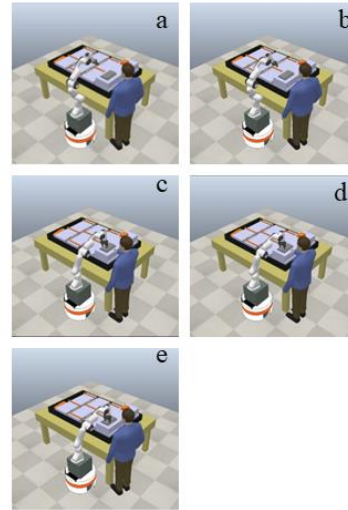


**FIGURE 11** ROBOT SPEED DURING MOVEMENT

FIGURE 12 shows the initial and final positions of case b), highlighting the movements made by the robot and the operator. The red arrows give a qualitative indication of the direction of motion of the end effector.



a) Start of motion b) End of motion

**FIGURE 12** OPERATOR AND ROBOT MOVEMENTS, CASE b)

FIGURE 13 shows the speed of the spheres used to represent the robot as a function of the distance measured between each of them and the dummy representing the operator. Again, the values obtained are compared with the maximum permissible speed according to ISO/TS 15066 (blue line).

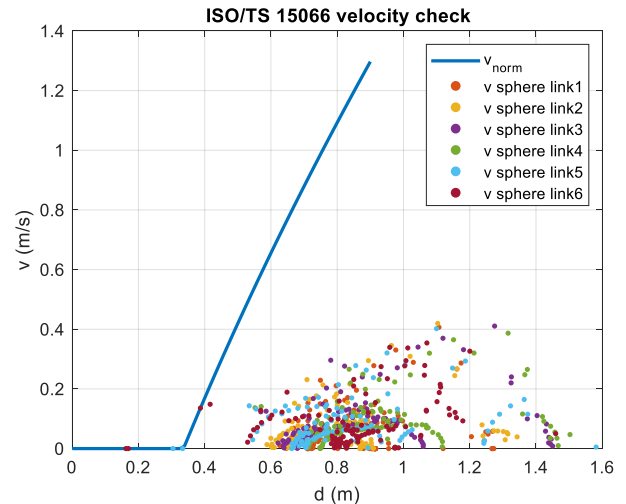


**FIGURE 13** SPEED OF THE ROBOT'S REPRESENTATIVE SPHERES AS A FUNCTION OF THE DISTANCE BETWEEN MAN AND ROBOT

## 8. DISCUSSION

The results of the simulations show that the control algorithms developed ensure at the same time that no potentially harmful collisions occur between man and robot, and that the robot can complete each planned task by sharing the workspace with man when necessary or appropriate.

The analysis of the possible disassembly cycles showed that this possibility significantly reduces the time needed to disassemble a battery pack, and thus contributes to the cost containment of this process.

Going into the details of the simulation results, it can be observed that in the first case analysed, shown in FIGURE 9, the mobile base to reach the final position (f) starting from the initial position (a). In a first step, the algorithm recognises the opportunity to follow a counterclockwise path to circumvent the table. Then, as shown in frames b, c, and d, it detects the presence of the operator in its path and deviates its trajectory to avoid him, passing behind him.

Throughout the entire path, the robot's speed remains below that prescribed by ISO/TS 15066.

The second case shows instead that the anthropomorphic robot starts its movement to reach the working position (frame a, b) and then retracts when the operator moves his arm occupying the same working space (frame c,d), and then returns to the working position when the operator withdraws his arm (frame e). Even in this case, the speed held by the robot in each of its parts remains below the maximum speed allowed by the standard, thus guaranteeing the safety of the interaction.

## 9. CONCLUSION

The results of this work indicate that proper planning of the battery pack disassembly process can limit the time required to perform the work. The process is faster if it is possible to plan stages during which the work space is shared between man and robot. This condition is only feasible if the safety of the operator can be guaranteed, i.e. that the robot cannot hit him under any conditions that could cause damage. The proposed collision control algorithms are based on the implementation of vision systems capable of detecting the position of the operator in real time, in the real case scenarios. Different versions have been developed, suitable for use in generating trajectories for a mobile platform, for an anthropomorphic robot and for the system consisting of the two. Their study in a simulation environment shows their ability to meet the requirements of ISO/TS 15066.

What has been achieved shows that the use of vision systems makes it possible to implement innovative ways of managing collaboration between humans and robots, laying the foundations for the development of applications in sectors where the complexity of the task and the number of different cases that need to be handled require the presence of a human operator to guarantee the necessary flexibility.

Future developments of this work concern the implementation of what is proposed in an experimental robotic cell and the execution of laboratory tests aimed at implementing the vision systems, as cameras for detecting the position of the human operator with respect to the robotic system and for improving the localization of the robots and its intuitive control [24], developing the trajectory generation algorithms and validating the complete system.

## ACKNOWLEDGEMENTS

The authors would like to thank INAIL - Istituto Nazionale per l'Assicurazione contro gli Infortuni sul Lavoro for supporting this research with the BRIC 2022 - ISACOB (Interazione Sicura e Autoadattativa tra uomo e robot COllaBorativo – Safe and autoadaptive interaction between man and collaborative robot) project

## REFERENCES

- [1] Q. Wei, Y. Wu, S. Li, R. Chen, J. Ding, and C. Zhang, "Spent lithium ion battery (LIB) recycle from electric vehicles: A mini-review," *Science of The Total Environment*, vol. 866, p. 161380, Mar. 2023, doi: 10.1016/j.scitotenv.2022.161380.
- [2] M. Melchiorre, L. Salamina, L. S. Scimmi, S. Mauro, and S. Pastorelli, "Experiments on the Artificial Potential Field with Local Attractors for Mobile Robot Navigation," *Robotics*, vol. 12, no. 3, Jun. 2023, doi: 10.3390/robotics12030081.
- [3] H. Poschmann, H. Brüggemann, and D. Goldmann, "Disassembly 4.0: A Review on Using Robotics in Disassembly Tasks as a Way of Automation," *Chemie Ingenieur Technik*, vol. 92, no. 4, pp. 341–359, Apr. 2020, doi: 10.1002/cite.201900107.
- [4] J. Li, M. Barwood, and S. Rahimifard, "A multi-criteria assessment of robotic disassembly to support recycling and recovery," *Resour Conserv Recycl*, vol. 140, pp. 158–165, Jan. 2019, doi: 10.1016/j.resconrec.2018.09.019.
- [5] J. Li, M. Barwood, and S. Rahimifard, "Robotic disassembly for increased recovery of strategically important materials from electrical vehicles," *Robotics and Computer-Integrated Manufacturing*, vol. 50. Elsevier Ltd, pp. 203–212, Apr. 01, 2018. doi: 10.1016/j.rcim.2017.09.013.
- [6] M. Marconi, G. Palmieri, M. Callegari, and M. Germani, "Feasibility Study and Design of an Automatic System for Electronic Components Disassembly," *Journal of Manufacturing Science and Engineering, Transactions of the ASME*, vol. 141, no. 2, Feb. 2019, doi: 10.1115/1.4042006.
- [7] S. Ruggeri, G. Fontana, V. Basile, M. Valori, and I. Fassi, "Micro-robotic Handling Solutions for PCB (re-)Manufacturing," *Procedia Manuf*, vol. 11, pp. 441–448, 2017, doi: 10.1016/j.promfg.2017.07.132.
- [8] I. Chatzikonstantinou, D. Giakoumis, and D. Tzouvaras, "A new shopfloor orchestration approach for collaborative human-robot device disassembly," in *Proceedings - 2019 IEEE SmartWorld, Ubiquitous Intelligence and Computing, Advanced and Trusted Computing, Scalable Computing and Communications, Internet of People and Smart City Innovation, SmartWorld/UIC/ATC/SCALCOM/IOP/SCI 2019*, Institute of Electrical and Electronics Engineers Inc.,

- Aug. 2019, pp. 225–230. doi: 10.1109/SmartWorld-UIC-ATC-SCALCOM-IOP-SCI.2019.00081.
- [9] K. Li, Q. Liu, W. Xu, J. Liu, Z. Zhou, and H. Feng, “Sequence planning considering human fatigue for human-robot collaboration in disassembly,” in *Procedia CIRP*, Elsevier B.V., 2019, pp. 95–104. doi: 10.1016/j.procir.2019.04.127.
- [10] A. Renteria and E. Alvarez-De-Los-Mozos, “Human-Robot Collaboration as a new paradigm in circular economy for WEEE management,” in *Procedia Manufacturing*, Elsevier B.V., 2019, pp. 375–382. doi: 10.1016/j.promfg.2020.01.048.
- [11] T. Elwert *et al.*, “Current developments and challenges in the recycling of key components of (Hybrid) electric vehicles,” *Recycling*, vol. 1, no. 1. MDPI AG, pp. 25–60, 2016. doi: 10.3390/recycling1010025.
- [12] X. Zhao, Y. Chen, L. Qian, B. Tao, and H. Ding, “Human–Robot Collaboration Framework Based on Impedance Control in Robotic Assembly,” *Engineering*, vol. 30, pp. 83–92, Nov. 2023, doi: 10.1016/j.eng.2022.08.022.
- [13] P. Palmieri, M. Melchiorre, L. S. Scimmi, S. Pastorelli, and S. Mauro, “Human Arm Motion Tracking by Kinect Sensor Using Kalman Filter for Collaborative Robotics,” 2021, pp. 326–334. doi: 10.1007/978-3-030-55807-9\_37.
- [14] L. S. Scimmi, M. Melchiorre, S. Mauro, and S. Pastorelli, “Experimental Real-Time Setup for Vision Driven Hand-Over with a Collaborative Robot,” in *2019 International Conference on Control, Automation and Diagnosis (ICCAD)*, IEEE, Jul. 2019, pp. 1–5. doi: 10.1109/ICCAD46983.2019.9037961.
- [15] M. Melchiorre, L. Sabatino Scimmi, S. Mauro, and S. Pastorelli, “Influence of Human Limb Motion Speed in a Collaborative Hand-over Task,” in *Proceedings of the 15th International Conference on Informatics in Control, Automation and Robotics*, SCITEPRESS - Science and Technology Publications, 2018, pp. 359–366. doi: 10.5220/0006864703590366.
- [16] E. Monari *et al.*, “Physical Ergonomics Monitoring in Human–Robot Collaboration: A Standard-Based Approach for Hand-Guiding Applications,” *Machines*, vol. 12, no. 4, p. 231, Mar. 2024, doi: 10.3390/machines12040231.
- [17] A. Raviola, R. Guida, A. C. Bertolino, A. De Martin, S. Mauro, and M. Sorli, “A Comprehensive Multibody Model of a Collaborative Robot to Support Model-Based Health Management,” *Robotics*, vol. 12, no. 3, Jun. 2023, doi: 10.3390/robotics12030071.
- [18] R. Guida, A. C. Bertolino, A. De Martin, A. Raviola, and M. Sorli “High Fidelity Modeling of Wear, Hysteresis, and Tooth Cracks in Strain Wave Gears for PHM Purposes,” *Proceedings of the ASME 2023 International Mechanical Engineering Congress and Exposition*, vol. 13, V013T15A022, New Orleans, Louisiana (USA), ASME, 2023, doi: 10.1115/IMECE2023-112537
- [19] M. Melchiorre, L. Scimmi, L. Salamina, S. Mauro, and S. Pastorelli, “Robot Collision Avoidance based on Artificial Potential Field with Local Attractors,” in *Proceedings of the 19th International Conference on Informatics in Control, Automation and Robotics*, SCITEPRESS - Science and Technology Publications, 2022, pp. 340–350. doi: 10.5220/0011353200003271.
- [20] J. F. Hellmuth, N. M. DiFilippo, and M. K. Jouaneh, “Assessment of the automation potential of electric vehicle battery disassembly,” *J Manuf Syst*, vol. 59, pp. 398–412, Apr. 2021, doi: 10.1016/j.jmsy.2021.03.009.
- [21] <https://www.autoweek.com/news/a38252667/battery-experts-explain-chevy-bolt-fires>; accessed on 15/7/2024
- [22] L. Salamina, M. Gaidano, M. Melchiorre, and S. Mauro, “Mobile robot with robotic arm: development and validation of a digital twin,” 2023. ASME International Mechanical Engineering Congress and Exposition. American Society of Mechanical Engineers, 2023. p. V003T03A064, DOI 10.1115/IMECE2023-113056
- [23] L. Sabatino Scimmi, M. Melchiorre, S. Mauro, and S. Pastorelli, “Multiple Collision Avoidance between Human Limbs and Robot Links Algorithm in Collaborative Tasks,” in *Proceedings of the 15th International Conference on Informatics in Control, Automation and Robotics*, SCITEPRESS - Science and Technology Publications, 2018, pp. 291–298. doi: 10.5220/0006852202910298.
- [24] A. Raviola, A. Coccia, A. De Martin, A.C. Bertolino, S. Mauro, M. Sorli “Development of a Human-Robot Interface for a Safe and Intuitive Telecontrol of Collaborative Robots in Industrial Applications,” in *Advances in Service and Industrial Robotics (RAAD 2022)*, Mechanisms and Machine Science, vol 120. Springer, 2022, doi:10.1007/978-3-031-04870-8\_65